RSC Advances

PAPER

View Article Online
View Journal | View Issue

Cite this: *RSC Adv.*, 2015, **5**, 37119

Unravelling the mechanism of the ketene-imine Staudinger reaction. An ELF quantum topological analysis†

Luis R. Domingo,* Mar Ríos-Gutiérrez and José A. Sáez

The mechanism of the ketene-imine Staudinger (KI-S) reaction between *t*-butyl-cyano ketene and *N*-phenyl phenylimine has been studied using DFT methods at the MPWB1K/6-311G(d) computational level. The reaction takes place through a two-step mechanism: (i) the first step is the nucleophilic attack of the imine nitrogen lone pair on the central carbon of the ketene yielding a zwitterionic (ZW) intermediate; (ii) the second step, which is the rate- and stereoselectivity-determining step, is a ring-closure process achieved by a nucleophilic attack of the terminal carbon atom of the ketene on the imine carbon atom. Due to the unfeasibility of a *cis*/*trans* and an *E*/*Z* stereoisomerisation at the ZW intermediates, *trans* and *cis* β-lactams are formed along the *endo* and *exo* stereoisomeric channels, respectively. An electron localisation function (ELF) quantum topological analysis of the bonding changes along the KI-S reaction permits a complete characterisation of the mechanism. The first step is associated with the formation of the N1–C4 single bond along the nucleophilic attack of the imine nitrogen lone pair on the central carbon of the ketene, while the second step is associated with a ring-closure process achieved by the C-to-C coupling of the C2 and C3 *pseudoradical centers* generated in the previous phases. The present theoretical study makes it possible to reject those analyses based on the FMO theory, in which HOMO/LUMO interactions along the nucleophilic attack of the imines on the ketenes and a feasible torquoelectronic effect along the conrotatory ring-closure step control the *cis*/*trans* stereoselectivity in the formation of β-lactams.

Received 25th February 2015
Accepted 13th April 2015

DOI: 10.1039/c5ra03438h

www.rsc.org/advances

Introduction

The β-lactam skeleton is the key structural element of the most widely employed family of antimicrobial agents to date, β-lactam antibiotics.[1] The first classical synthesis of molecules containing the β-lactam skeleton was the ketene-imine Staudinger (KI-S) reaction,[2] which is a formal [2 + 2] cycloaddition between a ketene **1** and an imine **2** yielding a β-lactam **4** (Scheme 1).[3,4]

A plethora of theoretical studies has been devoted to establish the mechanism of the KI-S reaction, as well as the stereoselectivity in the cyclisation step.[4,5] Originally, the KI-S reaction was classified as a pericyclic reaction. However, since [2 + 2] cycloadditions are forbidden and zwitterionic (ZW) intermediates were experimentally characterised, the pericyclic mechanism was quickly rejected. The accepted mechanism of the KI-S reaction is shown in Scheme 1. The reaction begins with the nucleophilic attack of imine **2** on the carbonyl carbon of ketene **1** to yield ZW intermediate **3**. The subsequent ring closure at this intermediate yields β-lactam **4**. This step has been associated with an electrocyclic reaction;[4,5a,d] consequently, a conrotatory electrocyclisation process at ZW intermediate **3** has

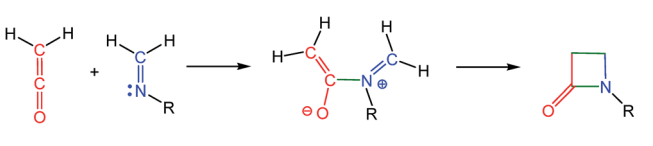

Scheme 1 Mechanism of the KI-S reaction.

Departamento de Química Orgánica, Universidad de Valencia, Dr Moliner 50, E-46100 Burjassot, Valencia, Spain. E-mail: domingo@utopia.uv.es; Web: http://www.luisrdomingo.com

† Electronic supplementary information (ESI) available: ELF topological analysis of bonding changes along the KI-S reaction between MCK **18** and *N*-methyl imine **19**, and of the stationary points involved in the *endo* stereoisomeric path of the KI-S reaction of TBCK **11** with *N*-phenyl imine **12a**. MPWB1K/6-311G(d) gas phase total and relative energies, total energies in benzene, and enthalpies, entropies and Gibbs free energies, computed at 80 °C and 1 atm in benzene, of the stationary structures involved in the reaction of TBCK **11** with *N*-phenyl imine **12a**. M062X/6-311G(d) Gibbs free energies and the relative ones, computed at 80 °C and 1 atm in benzene, of the most relevant stationary structures involved in the reaction of TBCK **11** with *N*-phenyl imine **12a**. MPWB1K/6-311G(d) total and relative energies, in benzene, of the stationary points along the *endo* and *exo* stereoisomeric channels associated with the KI-S reactions of *N*-phenyl imine **12a** with the monosubtituted ketenes **15a–c**. MPWB1K/6-311G(d) gas phase total and relative energies of the stationary structures involved in the reaction of MCK **18** with *N*-methyl imine **19**. Cartesian coordinates of all species involved in the studied KI-S reactions. See DOI: 10.1039/c5ra03438h

been proposed along the formation of β-lactams. The frontier molecular orbital (FMO) theory has been intensively used in order to explain both the mechanism and *cis*/*trans* stereoselectivity in KI-S reactions.

The reaction of unsymmetrical substituted ketenes and imines may form *cis* and *trans* β-lactams (see Scheme 2).[6] If only steric effects are considered, the preferred reactive channel is that in which the bulky substituent R1 of the ketene is located outward from the imine nitrogen atom, leading to *exo* ZW intermediates. Houk proposed that along the conrotatory electrocyclic reactions of butadienes torquoelectronic effects are responsible for the *inward* or *outward* movements.[7] Cossio suggested that the strong analogy observed in the torquoselectivity of KI-S reactions compared with the conrotatory electrocyclic reactions of butadienes supports the pericyclic reactivity of the ZW intermediates formed in the KI-S reaction.[4] Consequently, it has been assumed that from (*E*)-imines, *cis* β-lactams are usually expected.

The analysis of the electron density reorganisation to evidence the bonding changes along a reaction path is the most attractive method to characterise a reaction mechanism.[8] An appealing procedure that provides a straightforward connection between the electron density distribution and the chemical structure is the study of the quantum chemical topology of the electron density based on the electron localisation function (ELF) of Becke and Edgecombe.[9] In this sense, Silvi and Savin presented the ELF in a very chemical fashion, using their topological analysis as a chemical bonding model.[10]

An ELF quantum topological analysis along the intrinsic reaction coordinate[11] (IRC) curve associated with the ring-aperture of cyclobutene **5** yielding 1,3-butadiene **6** has revealed that the bonding changes along the one-step mechanism take place along five different phases, the electrocyclic reaction being non-concerted (see Scheme 3).[8b] This behaviour allows rejecting the proposed pericyclic mechanism[12] for this electrocyclic reaction.[13] In addition, as the reaction begins with the rupture of the C–C single bond, the analysis based on the symmetry of the p_z atomic orbital of butadiene should be rejected when explaining the conrotatory aperture.[14]

The selectivity in the formation of β- *vs.* δ-lactams in the KI-S reaction between chloro-cyano-ketene (CCK, **7**) and two phenyl substituted unsaturated imines **8a,b** has been studied very recently (see Scheme 4).[15] These reactions are initialised by the

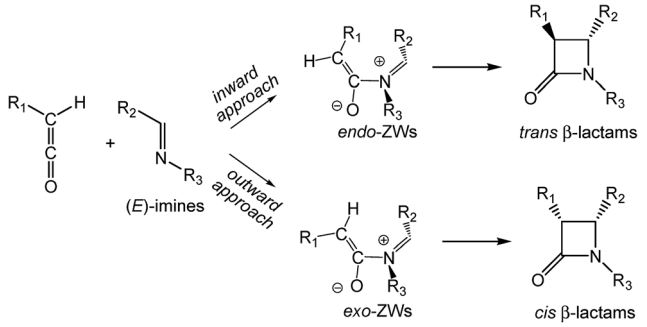

Scheme 2 Formation of *cis* and *trans* β-lactams in KI-S reactions.

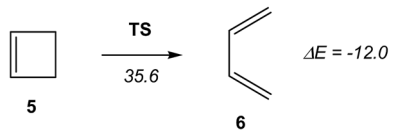

Scheme 3 Electrocyclic aperture of cyclobutene **5**. Energies are in kcal mol^{-1}.

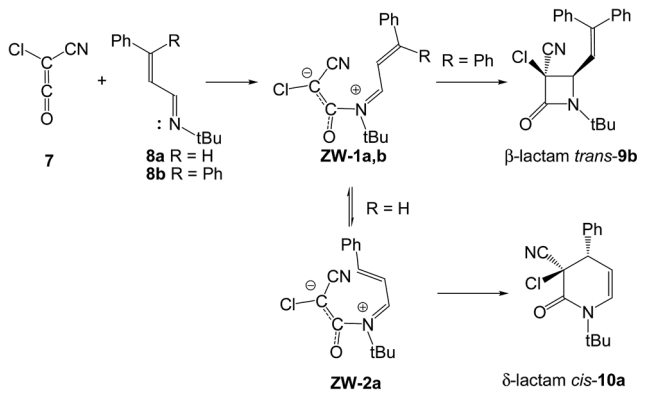

Scheme 4 KI-S reactions between CCK **7** and the unsaturated imines **8a,b**.

nucleophilic attack of unsaturated imines **8a,b** on ketene **7** with formation of ZW intermediates **ZW-1a,b**. The subsequent C–C single bond formation at the imine carbon or at the β-conjugated position enables the formation of β- or δ-lactams *trans*-**9b** or *cis*-**10a**, respectively. Due to the high electrophilic character of CCK **7**, $\omega = 2.20$ eV,[16] and the high nucleophilic character of these unsaturated imines, $N = 3.61$ eV (**8a**) and 3.74 eV (**8b**),[17] the nucleophilic attack did not present any activation barrier. Analysis of the energies involved in the two competitive channels associated with the ring-closure processes explained the selectivity experimentally observed; in the absence of any steric hindrance, formation of δ-lactam *cis*-**10a** is favoured over the formation of the corresponding β-lactam.

In addition, due to the structural behaviours of the ZW intermediates, in which the ketene and imine frameworks present a *quasi* perpendicular rearrangement, no specific rotation for the subsequent C–C single bond formation is required.[15] Consequently, formation of β-lactam *trans*-**9b** is determined by the *endo* approach mode of the cyano substituent of CCK **7** with respect to the nitrogen atom of the corresponding unsaturated imine **8b**. Therefore, no torquoelectronic processes take place in these KI-S reactions, as has been proposed.[4]

An ELF topological analysis of the bonding changes along the cyclisation step allowed establishing that the formation of the second C–C bond takes place through a retro-donation process involving the nucleophilically activated C–C double bond of the ketene and the electrophilically activated C–N or C–C double bond of the unsaturated imines. Thus, since the N–C single bond formed along the first step of the KI-S reaction does not participate in the cyclisation step, the electrocyclic mechanism was ruled out.[15]

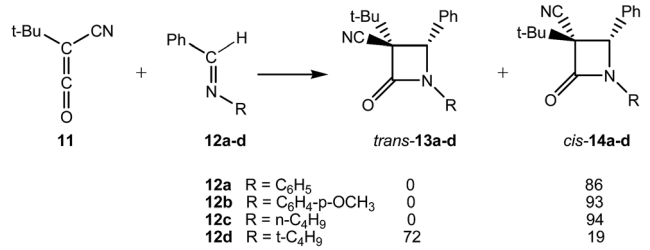

Scheme 5 KI-S reactions between TBCK **11** and N-substituted imines **12a–d**.

The KI-S reactions between *t*-butyl-cyano-ketene (TBCK, **11**) and N-substituted imines **12a–d** yielding the corresponding β-lactams *trans*-**13a–d** and/or *cis*-**14a–d** were experimentally studied by Moore (see Scheme 5).[18] The *cis*/*trans* stereoselectivity of these KI-S reactions was directly related to the steric bulk of the N-substituent of the imine. Generally, as this substituent increases in size, the yield of the resulting β-lactams having a *cis* relationship between the 3-cyano and 4-protio groups increases.[18]

For the KI-S reactions of TBCK **11** with N-substituted (*E*)-imines **12a,d**, Moore proposed that β-lactams *cis*-**14a** and *trans*-**13d** are formed through a conrotatory ring-closure in ZW intermediates (*Z*)-**ZW-3a** and (*E*)-**ZW-3d** (see Scheme 6).[18] These ZW intermediates are those in which steric interactions have been minimized, *i.e.* the smaller CN substituent of TBCK **11** is *endo* oriented and the larger *t*-Bu one is *exo* oriented. He proposed that the relative proportions of the (*E*) and (*Z*) ZW

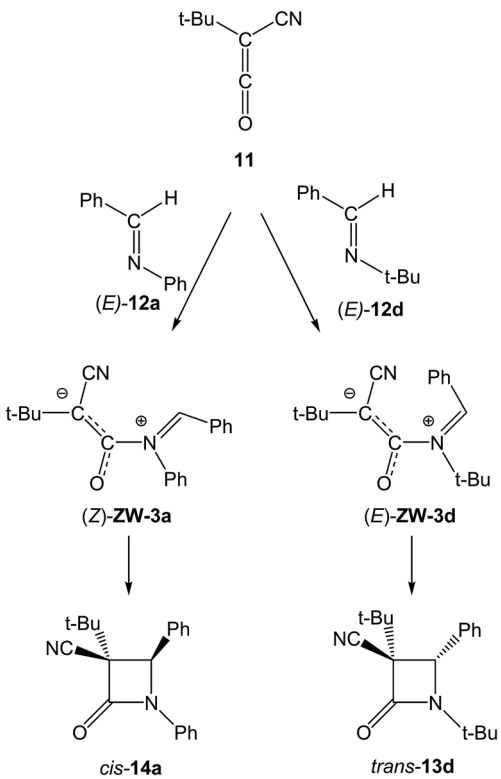

Scheme 6 Proposed origin of the *cis*/*trans* stereoselectivity in the KI-S reactions between TBCK **11** and N-substituted imines **12a,d**.[18]

intermediates, and thus also the corresponding β-lactams *trans*-**13d** and *cis*-**14a**, are significantly influenced by the bulk of the N-substituent. That is, when R is a small phenyl group, (*Z*)-**ZW-3a** is greatly favoured since the phenyl/cyano interaction is relieved, and thus β-lactams *cis*-**14a** results as the major or exclusive product. However, when R becomes a larger *t*-butyl group its steric interaction with the adjacent phenyl group increases, and thus the concentration of (*E*)-**ZW-3d** also increases.[18] Note that an *E*/*Z* isomerisation at the expected (*E*)-**ZW-3a** is demanded in this mechanism for the formation of β-lactam *cis*-**14a**.

Herein, the KI-S reaction between TBCK **11** and *N*-phenyl imine **12a**, experimentally studied by Moore,[18] yielding β-lactams *trans*-**13a** and/or *cis*-**14a** is investigated using DFT methods at the MPWB1K/6-311G(d) level in benzene (see Scheme 5). The aim of this theoretical study is to perform a complete characterisation of the molecular mechanism of the KI-S reaction. For this purpose, an ELF topological analysis of the bonding changes along the *endo* reactive channel associated with the KI-S reaction between methyl-cyano-ketene (MCK, **18**) and *N*-methyl imine **19**, as a reduced model of the KI-S reaction between TBCK **11** and imine **12a**, is carried out. In addition, the factors controlling the *endo*/*exo* selectivity are analysed.

Computational methods

DFT computations were carried out using the MPWB1K[19] exchange-correlation functional, together with the standard 6-311G(d) basis set.[20] The optimisations were performed using the Berny analytical gradient optimisation method.[21] The stationary points were characterised by frequency computations in order to verify that TSs have one and only one imaginary frequency. The IRC paths[11] were traced in order to check the energy profiles connecting each TS to the two associated minima of the proposed mechanism using the second order González–Schlegel integration method.[22] Solvent effects of benzene in the optimisations were taken into account using the polarisable continuum model (PCM) as developed by Tomasi's group[23] in the framework of the self-consistent reaction field (SCRF).[24] Values of enthalpies, entropies and free energies in benzene were calculated with the standard statistical thermodynamics at 80 °C and 1 atm.[20] The electronic structures of the stationary points were analysed by the natural bond orbital (NBO) method[25] and by the ELF topological analysis, $\eta(\mathbf{r})$.[9] The ELF study was performed with the TopMod program[26] using the corresponding monodeterminantal wavefunctions of the selected structures of the IRC. All computations were carried out with the Gaussian 09 suite of programs.[27]

The global electrophilicity index,[16] ω, is given by the following expression, $\omega = (\mu^2/2\eta)$, in terms of the electronic chemical potential μ and the chemical hardness η. Both quantities may be approached in terms of the one-electron energies of the frontier molecular orbitals HOMO and LUMO, ε_H and ε_L, as $\mu \approx (\varepsilon_H + \varepsilon_L)/2$ and $\eta \approx (\varepsilon_L - \varepsilon_H)$, respectively.[28] The global nucleophilicity index,[17] N, based on the HOMO energies obtained within the Kohn–Sham scheme,[29] is defined as $N = E_{HOMO}(Nu) - E_{HOMO}(TCE)$. This relative nucleophilicity index is referred to tetracyanoethylene (TCE).

Results and discussion

The present theoretical study has been divided into three parts: (i) first, energetic and geometrical details of the KI-S reaction between TBCK **11** and *N*-phenyl imine **12a** yielding β-lactams *trans*-**13a** and/or *cis*-**14a** are given; (ii) then, the origin of the *cis*/*trans* stereoselectivity in the KI-S reaction is analysed; finally (iii) an ELF topological analysis of the reaction between MCK **18** and *N*-methyl imine **19** is carried out in order to characterise the molecular mechanism of the KI-S reaction.

(i) Energy and geometry details of the KI-S reaction between TBCK 11 and *N*-phenyl imine 12a

Due to the unsymmetry of TBCK **11** and *N*-phenyl imine **12a**, two stereoisomeric approach modes, the *endo* and the *exo* ones, are feasible along the nucleophilic attack of imine **12a** on ketene **11**. They are related to the two stereoisomeric approach modes of the cyano group of TBCK **11** relative to the sp^2 hybridised N1 nitrogen of imine **12a**; along the *endo* channel, the cyano group is placed over the nitrogen atom of the imine framework. An exploration of the potential energy surface (PES) for this polar reaction allowed finding two TSs and one ZW intermediate along each stereoisomeric channel connecting both TSs, indicating that this reaction takes place through a two-step mechanism. Consequently, the reagents, two TSs, one ZW intermediate and the corresponding β-lactam were located and characterised along each stereoisomeric channel (see Scheme 7). Relative energies in benzene of the stationary points associated with this KI-S reaction are given in Table 1, while the total electronic energies are given in Table S4 in the ESI.† Gas phase electronic energies are given in Table S3 in the ESI.†

The activation energies associated with the nucleophilic attack of the N1 nitrogen of *N*-phenyl imine **12a** on the C4 carbon of TBCK **11** in benzene are 2.2 (**TS1-4n**) and 13.8 (**TS1-4x**) kcal mol^{-1}; formation of the ZW intermediate resulting from the *endo* approach mode, **ZW-4n**, is exothermic by 4.8 kcal mol^{-1}, while formation of the ZW intermediate resulting from the *exo* one, **ZW-4x**, is endothermic by 4.5 kcal mol^{-1}. The activation energy associated with the C3–C4 and N1–C2 bond rotations at **ZW-4n** has been estimated to be *ca.* 32 and 34 kcal mol^{-1}. These unfavourable energies prevent the *endo*/*exo* and the *E*/*Z* isomerisations at **ZW-4n**, respectively. These ZW intermediates undergo a cyclisation process yielding β-lactams *trans*-**13a** and *cis*-**14a** with an activation energy of 16.7 (**TS2-4n**) and 15.5 (**TS2-4x**) kcal mol^{-1}. The KI-S reaction is strongly exothermic, between −34 and −38 kcal mol^{-1}.

Table 1 MPW1K/6-311G(d) relative[a] electronic energies (Δ*E*, in kcal mol^{-1}) in benzene, and enthalpies (Δ*H*, in kcal mol^{-1}), entropies (Δ*S*, in cal mol^{-1} K^{-1}) and Gibbs free energies (Δ*G*, in kcal mol^{-1}), computed at 80 °C and 1 atm in benzene, of the stationary structures involved in the KI-S reaction of TBCK **11** with *N*-phenyl imine **12a**

	Δ*E*	Δ*H*	Δ*S*	Δ*G*
TS1-4n	2.2	3.1	−43.1	18.3
TS1-4x	13.8	14.9	−43.7	30.3
ZW-4n	−4.8	−2.5	−46.8	14.0
ZW-4x	4.5	6.9	−51.8	25.2
TS2-4n	11.9	13.1	−53.2	31.8
TS2-4x	20.0	21.0	−52.4	39.5
trans-**13a**	−34.1	−30.6	−54.1	−11.5
cis-**14a**	−38.0	−34.8	−51.2	−16.8

[a] Relative to TBCK **11** and *N*-phenyl imine **12a**.

Some interesting conclusions can be drawn from these energy results: (i) the nucleophilic attack of *N*-phenyl imine **12a** on TBCK **11** is completely *endo* stereoselective, **TS1-4x** being 11.6 kcal mol^{-1} higher in energy than **TS1-4n**; (ii) while formation of **ZW-4n** is exothermic by *ca.* 5 kcal mol^{-1}, formation of **ZW-4x** is endothermic by *ca.* 5 kcal mol^{-1}; (iii) the **ZW-4n**/**ZW-4x** isomerisation *via* the C3–C4 bond rotation is found to be very unfavourable; (iv) the ring-closure along the *exo* stereoselective channel is found slightly less energetic than that along the *endo* one. However, as **ZW-4n** is located 9.3 kcal mol^{-1} below **ZW-4x**, **TS2-4n** is found 8.1 kcal mol^{-1} below **TS2-4x**; (v) the formation of β-lactams *trans*-**13a** and *cis*-**14a** is strongly exothermic; finally, (vi) the very high energy associated with the N1–C2 bond rotation at **ZW-4n** allows discarding Moore's proposal for the formation of β-lactam *cis*-**14a** from (*E*)-*N*-phenyl imine **12a** (see Scheme 6).[18]

Relative enthalpies, entropies and Gibbs free energies of the stationary points involved in the KI-S reaction of TBCK **11** with

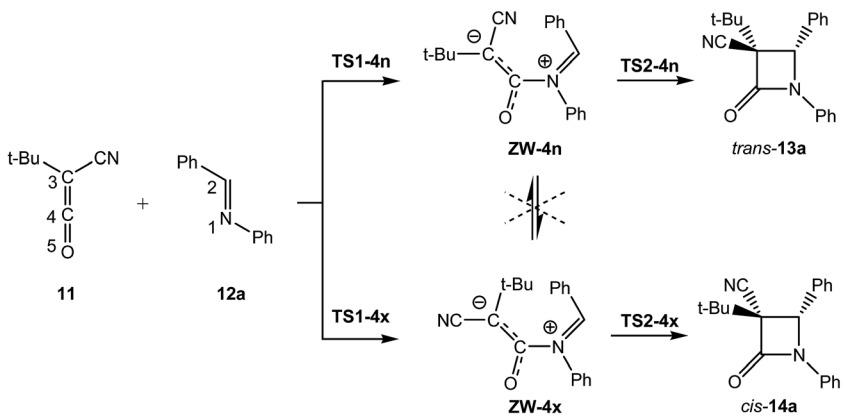

Scheme 7 Mechanism of the KI-S reaction between TBCK **11** and *N*-phenyl imine **12a**.

N-phenyl imine **12a** are given in Table 1. Enthalpies, entropies and Gibbs free energies of the stationary points associated with this KI-S reaction are given in Table S4 in the ESI.† The addition of the thermal corrections to the electronic energies increases the activation and reaction enthalpies between 1 and 4 kcal mol^{-1}. The addition of the entropies to enthalpies raises relative Gibbs free energies between 15–19 kcal mol^{-1} due to the unfavourable entropy associated with this bimolecular reaction. Thus, the activation Gibbs free energy associated with the nucleophilic attack of *N*-phenyl imine **12a** on TBCK **11** increases to 18.3 (**TS1-4n**) and 30.3 (**TS1-4x**) kcal mol^{-1}; formation of ZW intermediates being endergonic by 14.0 (**ZW-4n**) and 25.2 (**ZW-4x**) kcal mol^{-1}. From these ZW intermediates the activation Gibbs free energy associated with the C2–C3 single bond formation along the ring-closure process is 17.8 (**TS2-4n**) and 14.3 (**TS2-4x**) kcal mol^{-1}. Formation of β-lactams *trans*-**13a** and *cis*-**14a** is exergonic by 11.5 and 16.8 kcal mol^{-1}, respectively.

A schematic representation of the Gibbs free energy profile of the two stereoisomeric channels associated with the KI-S reaction of TBCK **11** with *N*-phenyl imine **12a** is given in Fig. 1. Some appealing conclusions can be drawn from these Gibbs free energy profiles: (i) due to the endergonic character of the formation of ZW intermediates **ZW-4n** and **ZW-4x**, the second step of this stepwise mechanism is the rate- and stereoisomeric-determining step of the reaction; (ii) consequently, the activation Gibbs free energy of this KI-S reaction along the most favourable *endo* channel is 31.8 kcal mol^{-1}; (iii) the reaction is kinetically *endo* selective, **TS2-4x** being 7.7 kcal mol^{-1} higher in energy than **TS2-4n**; (iv) β-lactam *cis*-**14a** is 5.3 kcal mol^{-1} thermodynamically more stable than β-lactam *trans*-**13a**; (v) these data indicate that while β-lactam *trans*-**13a** is the kinetic control product, β-lactam *cis*-**14a** is the thermodynamic control product; and (vi) the activation Gibbs free energy of the retro KI-S reaction from β-lactam *trans*-**13a**, 43.3 kcal mol^{-1}, is slightly higher than that associated with the formation of β-lactam *cis*-**14a**, *via* **TS2-4x**, 39.5 kcal mol^{-1}. Therefore, under thermodynamic control, β-lactam *cis*-**14a** becomes the product of this KI-S reaction.

In order to support the MPWB1K energy results for the thermodynamic control in the formation of β-lactam *cis*-**14a**, the Gibbs free energies of the most significant stationary points involved in the formation of the β-lactams *trans*-**13a** and *cis*-**14a** were computed using the M062X functional.[30] Thermodynamic data are given in Table S5 in the ESI.† Analysis of the relative M062X/6-311G(d) Gibbs free energies shows a similar trend to that obtained at the MPWB1K/6-311G(d) level. The activation Gibbs free energy associated with the formation of β-lactam *trans*-**13a**, *via* **TS2-4n**, is 29.7 kcal mol^{-1}, formation of *trans*-**13a** is exergonic by 12.3 kcal mol^{-1}. β-Lactam *cis*-**14a** is 4.4 kcal mol^{-1} more stable than β-lactam *trans*-**13a**. Consequently, *cis*-**14a** is the product of a thermodynamic control. The activation Gibbs free energy associated with the retro KI-S reaction from *trans*-**13a** is 42.0 kcal mol^{-1}, *i.e.* 4.7 kcal mol^{-1} higher than the activation Gibbs free energy associated with the formation of β-lactam *cis*-**14a** *via* **TS2-4x**. Similar to the MPWB1K results, if the retro KI-S reaction is reached, β-lactam *cis*-**14a** becomes the thermodynamic control product.

The geometries of the TSs involved in the KI-S reaction between TBCK **11** and *N*-phenyl imine **12a** are given in Fig. 2. The lengths of the N1–C4 and C2–C3 forming bonds along the nucleophilic attack of imine **12a** on TBCK **11** in benzene are 2.124 and 3.507 Å at **TS1-4n**, and 2.040 and 3.692 Å at **TS1-4x**. At the ZW intermediates the length of the N1–C4 single bond is 1.530 Å (**ZW-4n**) and 1.518 Å (**ZW-4x**), while the distance between the C2 and C3 atoms remains at 3.111 Å (**ZW-4n**) and 3.167 Å (**ZW-4x**). Remarkably, at **ZW-4n** and **ZW-4x**, the ketene and the imine frameworks are not completely perpendicular; at these intermediates the N1–C4–C3–C2 dihedral angle is −75.6 degrees at **ZW-4n** and −79.1 degrees at **ZW-4x**. This slight twist enables the approach of the C3 carbon of the ketene framework towards the C2 carbon of the imine one, thus favouring the

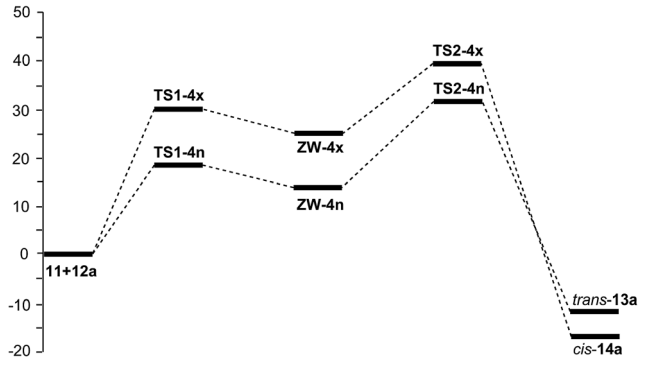

Fig. 1 MPWB1K/6-311G(d) Gibbs free energy profile, in kcal mol^{-1}, of the KI-S reaction between TBCK **11** and *N*-phenyl imine **12a** in benzene.

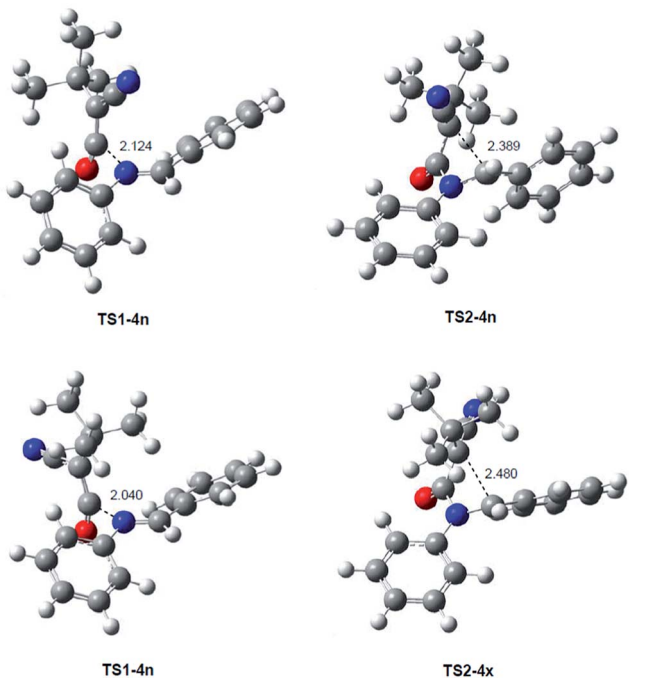

Fig. 2 MPWB1K/6-311G(d) geometries, in benzene, of the TSs associated with the KI-S reaction between TBCK **11** and *N*-phenyl imine **12a**.

subsequent cyclisation process.[15] At the TSs associated with the formation of the β-lactams, the length of the C2–C3 bond is 2.389 Å at **TS2-4n** and 2.480 Å at **TS2-4x**, while the length of the N1–C4 single bond has decreased to 1.439 Å at **TS2-4n** and 1.430 Å at **TS2-4x**.

The polar nature of this KI-S reaction was analysed by computing the global electron density transfer (GEDT). The natural atomic charges at the TSs and intermediates for the *endo*/*exo* channels, obtained through a natural population analysis (NPA), were shared between the ketene and the imine frameworks. In benzene, the GEDT that fluxes from the imine framework to the ketene one is 0.20e at **TS1-4n**, 0.55e at **ZW-4n** and 0.29e at **TS2-4n** along the *endo* approach mode, and 0.23e at **TS1-4x**, 0.55e at **ZW-4x** and 0.30e at **TS2-4x** along the *exo* one. These values indicate that along this stepwise reaction there is an increase of the GEDT along the nucleophilic attack of *N*-phenyl imine **12a** on ketene **11**, reaching the maximum value with the formation of the N1–C4 single bond at the corresponding ZW intermediates. The very high GEDT found at these intermediates points to their high ZW character and their great stability, in clear agreement with the high electrophilic character of TBCK **11**, $\omega = 1.36$ eV, and the high nucleophilic character of *N*-phenyl imine **12a**, $N = 3.36$ eV. From these ZW intermediates to the β-lactams there is a GEDT decrease as a consequence of a retro-donation along the ring-closure process.

(ii) Origin of the cis/trans selectivity in the KI-S reaction

As commented in the introduction, the KI-S reaction of unsymmetrically substituted ketenes and imines may form *cis* and *trans* β-lactams (see Scheme 2). The unsymmetric substitution in ketenes, as in CCK **7** and TBCK **11**, opens up the feasibility of two reactive channels along the approach of the imine nitrogen atom towards the central carbon atom of the ketene. Taking the group of higher importance of the ketene (HG) as reference, these approach modes can be named *endo* and *exo* (see Scheme 8).

The substituents present in the ketene can be classified as electron-withdrawing (EW) substituents able to increase the electrophilic character of the ketene, herein named *type I*, and bulky hydrocarbon substituents, herein named *type II*. Along the nucleophilic attack of the imine on the ketene, substituents *type I* can electronically interact with the imine nitrogen atom favouring the *endo* approach mode, while the unfavourable steric hindrance generated by a bulky hydrocarbon substituent *type II* favours the *exo* approach mode. In the case of disubstituted ketenes such as TBCK **11** the CN substituent *type I* prefers the *endo* approach mode, while the bulky *t*-butyl substituent *type II* prefers the *exo* one.

In order to analyse the effects of the ketene substitution in the *endo*/*exo* stereoselectivity along the KI-S reaction, the two stereoisomeric reaction channels associated with the nucleophilic attack of *N*-phenyl imine **12a** on the monosubstituted ketenes **15a–c** were studied (see Scheme 9). The relative energies of the stationary points associated with these KI-S reactions in benzene are given in Table 2, while the total electronic energies are given in Table S6 in the ESI.†

When the ketene substituent is *type I*, R = CN, *endo* **TS1-5an** is located 1.5 kcal mol^{-1} below *exo* **TS1-5ax**. This low energy difference indicates that electronic factors have a low effect on the *endo*/*exo* stereoselectivity along the first step of the KI-S reactions. However, when the ketene substituent is *type II*, a bulky *t*-butyl group, a considerable effect on the stereoselectivity is observed; note that *endo* **TS1-5cn** is located 6.8 kcal mol^{-1} above *exo* **TS1-5cx**. Finally, for the small methyl group, *endo* **TS1-5bn** is located only 0.20 kcal mol^{-1} above *exo* **TS1-5bx**. Consequently, steric hindrances along the *endo* approach mode have a stronger effect on the stereoselectivity than electronic factors.

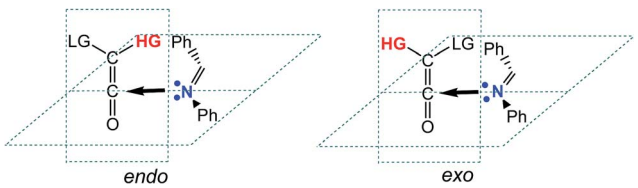

Scheme 8 *Endo* and *exo* stereoisomeric approach modes of the group of higher importance (HG) over the imine nitrogen atom. The LG group corresponds to the group of lower importance.

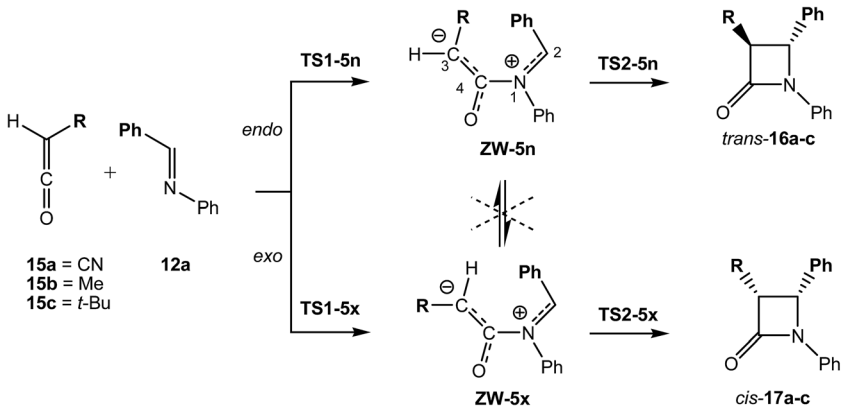

Scheme 9 Mechanism of the KI-S reaction between ketenes **15a-b** and *N*-phenyl imine **12a**.

Table 2 MPWB1K/6-311G(d) relative energies (in kcal mol^{-1}) in benzene of the stationary points along the *endo* and *exo* stereoisomeric channels associated with the KI-S reactions of *N*-phenyl imine **12a** with the monosubtituted ketenes **15a–c**

CN	ΔE	Me	ΔE	*t*-Bu	ΔE
TS1-5an	−1.2	**TS1-5bn**	8.0	**TS1-5cn**	16.7
TS1-5ax	0.2	**TS1-5bx**	7.8	**TS1-5cx**	9.9
ZW-5an	−6.5	**ZW-5bn**	8.0	**ZW-5cn**	14.4
ZW-5ax	−4.6	**ZW-5bx**	6.3	**ZW-5cx**	8.0
TS2-5an	14.2	**TS2-5bn**	21.4	**TS2-5cn**	27.1
TS2-5ax	11.7	**TS2-5bx**	14.1	**TS2-5cx**	16.0
trans-**16a**	−38.4	*trans*-**16b**	−44.7	*trans*-**16c**	−43.5
cis-**17a**	−37.4	*cis*-**17b**	−44.5	*cis*-**17c**	−39.6

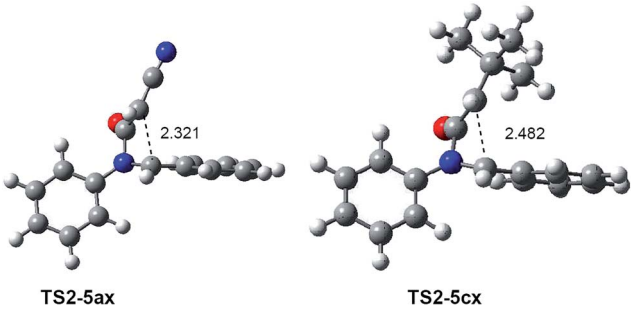

Fig. 3 MPWB1K/6-311G(d) geometries of the most favourable *exo* TSs associated with the ring-closure step of the KI-S reactions of *N*-phenyl imine **12a** with the monosubstituted ketenes **15a,c**.

Along the second step of the KI-S reaction, only steric effects seem to control the ring-closure process. Thus, substituents *type II* yield *endo* ring-closure activation energies being 5.6 (**TS2-5bn**) and 4.7 (**TS2-5cn**) kcal mol^{-1} higher than the *exo* ones. Interestingly, for substituents *type I* there is a selectivity change, *i.e.* the ring-closure along the *exo* channel is 4.4 (**TS2-5ax**) kcal mol^{-1} lower in energy than the *endo* one. Consequently, along the second step of the KI-S reaction, the *exo* approach mode of the bulkier substituent is the preferred one. When the energies of the TSs are referenced to the separated reagents, the *exo* approach mode is 2.5 (**TS2-5ax**) 7.3 (**TS2-5bx**) and 11.1 (**TS2-5cx**) kcal mol^{-1} more favourable than the *endo* one.

Analysis of the electronic and steric effects in the *endo*/*exo* stereoselectivity along the nucleophilic attack of imines to ketenes, and the subsequent ring-closure at the corresponding ZW intermediates permits to conclude that the steric hindrance provoked by bulky substituents may be the main factor controlling the *cis*/*trans* stereoselectivity of KI-S reactions under kinetic control.

This analysis of the *endo*/*exo* selectivity in the KI-S reactions is in agreement with the *endo* selectivity found in the experimental reaction of TBCK **11** with *N*-phenyl imine **12a**, in which the *endo* TSs **TS1-4n** and **TS2-4n** are found *ca.* 10 kcal mol^{-1} below the *exo* ones (see Fig. 1). Note that along the most favourable *endo* reactive channel the bulky *t*-butyl group is placed in an *exo* disposition with respect to the imine nitrogen atom.

The geometries of the most favourable *exo* TSs associated with the ring-closure step of the KI-S reaction of *N*-phenyl imine **12a** with the monosubstituted ketenes **15a,c** are given in Fig. 3. The geometries of **TS2-5ax** and **TS2-5cx** resemble those of the corresponding *exo* ZW intermediates. In both TSs, the ketene framework is slightly twisted in order to approach the C2 and the C3 carbons, while the *N*-phenyl imine framework remains almost unchanged. Therefore, neither conrotatory/disrotatory nor *inward* or *outward* movements take place along the ring-closure process, as has been proposed.[4]

The N1–C2 and C3–C4 bond order (BO) values at the most favourable zwitterionic intermediates are: 1.59 and 1.43 at **ZW-5an**, 1.61 and 1.61 at **ZW-5bx**, and 1.61 and 1.61 at **ZW-5cx**; these values suggest that these bonds have a high double bond character (see later). This behaviour is a consequence of the fact that along the nucleophilic attack of the N1 nitrogen atom on the C4 carbon atom of the ketene, the two N1–C2 and C3–C4 double bonds do not participate directly in the process (see later). These high BO values together with the high activation energy estimated for the N1–C2 and C3–C4 bond rotations at **ZW-5an**, higher than *ca.* 34 kcal mol^{-1}, indicate that along these KI-S reactions neither *E*/*Z* nor *cis*/*trans* isomerisations are feasible.

Consequently, *trans* β-lactams are obtained along the *endo* stereoisomeric channels, while *cis* β-lactams are obtained along the *exo* ones. Summing up, it can be concluded that the *cis*/*trans* stereoselectivity of the KI-S reaction is kinetically controlled by steric factors along the C–C bond formation in the ring-closure step.

For the KI-S reaction between TBCK **11** and imine **12a** in benzene, the present theoretical study permits to conclude that β-lactam *trans*-**13a** is the kinetic product, but Moore suggested by means of a H-NMR structural analysis that β-lactam *cis*-**14a** is the experimentally obtained product.[18] The present theoretical study also indicates that experimental β-lactam *cis*-**14a** should be formed *via* **TS2-4x**, in which the bulky *t*-butyl group is *endo* with respect to the imine framework, a very unfavourable rearrangement being in clear agreement with the high energy of **TS2-4x** with respect to **TS2-4n**, *ca.* 8 kcal mol^{-1}. On the other hand, β-lactam *cis*-**14a** could come from (*Z*)-**ZW-3a** as Moore proposed (see Scheme 6).[18] However, the high energy associated with the *E*/*Z* isomerisation allows ruling out the formation of ZW intermediate (*Z*)-**ZW-3a**. β-lactam *cis*-**14a** is found *ca.* 4 kcal mol^{-1} thermodynamically more stable than β-lactam *trans*-**13a**. Analysis of the Gibbs free energy profile of the KI-S reaction between TBCK **11** and imine **12a** indicates that a thermodynamic control of the reaction is possible, favouring the formation of the experimental β-lactam *cis*-**14a**. These results suggest that the analysis of the *cis*/*trans* stereoselectivity in a KI-S reaction may be far more complex than a simple kinetic study.

(iii) ELF topological analysis of the KI-S reaction

A great deal of work has emphasised that the ELF topological analysis along a reaction path is a valuable tool to understand the bonding changes along the reaction path, and thus to characterise the molecular mechanism.[8] After an analysis of the electron density, ELF provides basins which are the domains in

which the probability of finding an electron pair is maximal.[31] The basins are classified as core and valence basins. The latter are characterised by the synaptic order, *i.e.* the number of atomic valence shells in which they participate.[32] Thus, there are monosynaptic, disynaptic, trisynaptic basins and so on. Monosynaptic basins, labelled V(A), correspond to lone pairs or non-bonding regions, while disynaptic basins, labelled V(A,B), connect the core of two nuclei A and B and, thus, correspond to a bonding region between A and B. This description recovers the Lewis bonding model, providing a very suggestive graphical representation of the molecular system.

The ELF topological analysis along the cyclisation of the zwitterionic intermediate **ZW-1b** giving β-lactam *trans*-**9b** allowed establishing that formation of the C–C bonds takes place through a retro-donation process involving the nucleophilically activated C–C double bond of the ketene and the electrophilically activated C–N double bond of the unsaturated imine (see Scheme 4).[15]

In order to gain insight into the complete characterisation of the molecular mechanism of the KI-S reaction, an ELF topological analysis of the bonding changes along the two reaction paths associated with the stepwise mechanism of the KI-S reaction between MCK **18** and *N*-methyl imine **19**, yielding β-lactam *trans*-**20**, was performed (see Scheme 10). In this KI-S reaction the bulky *t*-butyl group present in TBCK **11** has been replaced by a methyl group in **18**, and the *N*-phenyl substituent present in imine **12a** has been replaced by a methyl group in **19**. From an ELF topological view, neither group substitution alters any obtained conclusion. The gas phase energies of the stationary points involved in this stepwise reaction are given in Table S7 in the ESI.† In addition, an ELF topological analysis of the stationary points involved in the *endo* stereoisomeric path of the KI-S reaction between TBCK **11** and *N*-phenyl imine **12a** is also performed. Details of these ELF topological analyses are also given in the ESI.† The attractor positions of the ELF for the most relevant points associated with the N1–C4 and C2–C3 bond formation along the two-step KI-S reaction between MCK **18** and *N*-methyl imine **19** are given in Fig. 4, while the basin population changes along the two steps of this KI-S reaction are graphically represented in Fig. 5.

Some appealing conclusions can be drawn from the ELF topological analysis of the KI-S reaction between MCK **18** and *N*-methyl imine **19**: (i) along step I, only four differentiated phases associated with the formation of the N1–C4 single bond are observed (see Fig. 5); (ii) formation of the N1–C4 single bond takes place in the last *Phase IV*, at *ca.* 1.67 Å, by sharing the electron density of the imine N1 lone pair with the ketene C4 carbon (see the V(N1,C4) disynaptic basin, integrating 2.15e, in

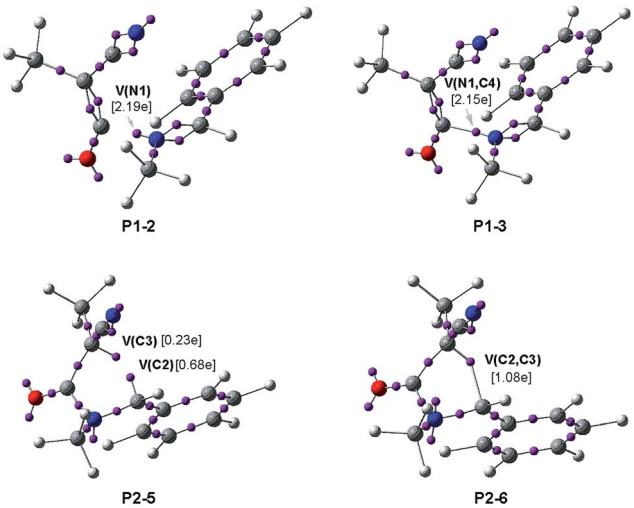

Fig. 4 ELF attractor positions of the most relevant points associated with the N1–C4 and C2–C3 bond formation along the two-steps KI-S reaction between MCK **18** and *N*-methyl imine **19**. The electron populations, in e, are given in brackets.

structure **P1–3** in Fig. 4, and the change from V(N1), in red in **P1–2**, to V(N1,C4), in blue in **P1–3**, in Fig. 5); (iii) along this step, while the N1–C2 and C3–C4 double bond regions remain characterised by the presence of two pairs of disynaptic basins, the C4–O5 bonding region of MCK **18** is depopulated in order to permit the N1–C4 single bond formation; (iv) along the nucleophilic attack of *N*-methyl imine **19** on MCK **18**, there is a GEDT increase until reaching a maximum value with the complete formation of N1–C4 at ZW intermediate **ZW-6n**, 0.54e; (v) at ZW intermediate **ZW-6n**, the N1–C2 and C3–C4 bonding regions are characterised by the presence of two disynaptic basins in each region (see **ZW-6n** in Fig. 5). This behaviour accounts for the high activation energy associated with the N1–C2, 44.6 kcal mol^{-1}, and C3–C4, 39.1 kcal mol^{-1}, bond rotations, which prevent *E*/*Z* imine and *cis*/*trans* ketene isomerisations. Note that these high rotational energies are similar to those found for the rotation of the N1–C2 and C3–C4 bonds at *endo* **ZW-4n**; (vi) along step II seven phases are observed (see Fig. 5); (vii) in *Phase II* and *Phase III*, only bonding changes in the C3–C4 and N1–C2 regions take place in order to create the monosynaptic basin V(C2) in *Phase V* and the monosynaptic basin V(C3) in *Phase VI*, which are demanded for the formation of the second C2–C3 single bond;[33] (viii) in *Phase IV* a new V(N1) monosynaptic basin appears, which reaches a maximum population in *Phase VI*. The electron density of this basin comes from the depopulation of the V(N1,C2) disynaptic basin. These changes are associated

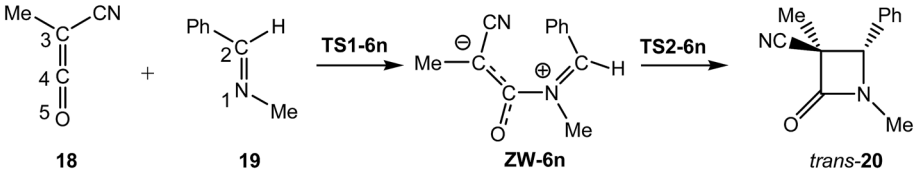

Scheme 10 Mechanism of the KI-S reaction between MCK **18** and *N*-methyl imine **19**.

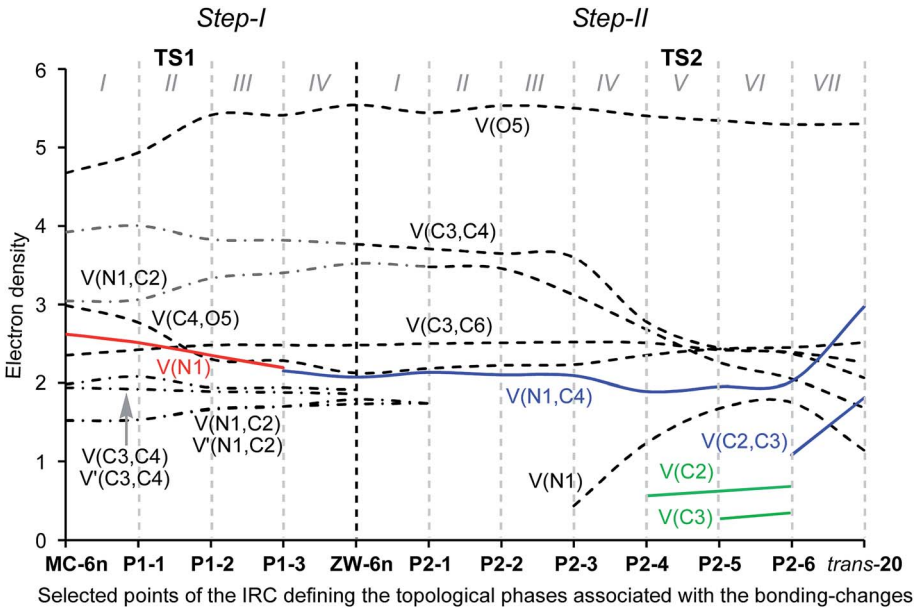

Fig. 5 Graphical representation of the basin-population changes along the two-step KI-S reaction between MCK **18** and *N*-methyl imine **19**. Point-dotted curves in grey represent the sum of the V(C*x*,C*y*) and V′(C*x*,C*y*) disynaptic basins describing a C–C double bond region.

with the formation of the new V(C2) monosynaptic basin in *Phase V*; (ix) formation of the C2–C3 single bond takes place at *Phase VII*, at a C2–C3 length of 2.079 Å, through the C-to-C coupling of the C2 and C3 *pseudoradical centers* generated in the previous phases (see the V(C2) and V(C3) monosynaptic basins, integrating 0.68e and 0.23e, respectively, in structure **P2–5** and the V(C2,C3) disynaptic basin, integrating 1.08e, in structure **P2–6** in Fig. 4);[33] (x) along step II, the GEDT decreases as a consequence of a retro-donation process associated with the formation of the C2–C3 single bond; (xi) along the ring-closure step, no specific N1–C2 and C3–C4 bond rotation takes place along the C2–C3 bond formation; and finally, (xii) a comparison of the ELF of the stationary points involved in the KI-S reaction between TBCK **11** and imine **12a**, and those involved in the reaction between MCK **18** and *N*-methyl imine **19** shows only small changes in the integration of the basins as a consequence of the different substitution in both reagents.

Conclusions

The mechanism of the KI-S reaction of TBCK **11** with *N*-phenyl imine **12a**, yielding β-lactams *trans*-**13a** and/or *cis*-**14a** has been studied using DFT methods at the MPWB1K/6-311G(d) level. This KI-S reaction takes place through a two-step mechanism: (i) the first step is the nucleophilic attack of the imine nitrogen lone pair on the central carbon of the ketene yielding a ZW intermediate; (ii) the second step is a ring-closure process achieved by the nucleophilic attack of the terminal carbon atom of the ketene on the imine carbon atom.

Along the first step, the imine molecule approaches the ketene in an almost perpendicular fashion until forming the corresponding ZW intermediates. This behaviour causes the subsequent ring-closure to take place through a slight movement in order to approach the two nucleophilic/electrophilic carbons of the ZW intermediate.[15] Consequently, neither a conrotaroty/disrotatory movement nor torquoelectronic effects along the ring-closure, as has been proposed,[4] take place. In addition, due to the double bond character of the imine C=N and ketene C=C bonds at the ZW intermediates, neither *E*/*Z* imine nor *cis*/*trans* ketene isomerisations are feasible.

Analysis of the Gibbs free energy profile of the reaction between TBCK **11** and *N*-phenyl imine **12a** indicates that the second step is the rate- and stereoselectivity-determining step of the KI-S reaction. Due to the unfeasibility of the *E*/*Z* imine and *cis*/*trans* ketene stereoisomerisation at the ZW intermediates, formation of *trans* and/or *cis* β-lactams depends on the relative Gibbs free energies of the *endo*/*exo* TSs associated with the ring-closure process, and not on the *endo*/*exo* approach mode along the first step of the reaction. This analysis indicates that while β-lactam *trans*-**13a** is the kinetic control product, the experimental β-lactam *cis*-**14a** should proceed from a thermodynamic control.

Analysis of the *endo*/*exo* stereoselectivity along the KI-S reaction of three monosubstituted ketenes, NC-, Me- and *t*-Bu-, indicates that steric hindrances are the main factor controlling the *endo*/*exo* stereoselectivity at the second reaction step and, consequently, the kinetic formation of *cis*/*trans* β-lactams.

An ELF quantum topological analysis of the bonding changes along the reaction between MCK **18** with *N*-methyl imine **19** permits a complete characterisation of the mechanism of the KI-S reaction. The first step is topologically very simple. Formation of the N–C single bond takes place in the last *Phase III*, at *ca.* 1.67 Å, by sharing the electron density of the imine nitrogen lone pair with the ketene central carbon. Along this step, while the imine N–C and ketene C–C double bond regions

remain topologically characterised by the presence of two pairs of disynaptic basins, the ketene C–O bonding region of MCK **18** is depopulated in order to permit the N–C single bond formation. Along the first step there is a GEDT increase until reaching a maximum value with the formation of the corresponding ZW intermediate, 0.54e.

At the ZW intermediate, the imine N–C and ketene C–C bonding regions are characterised by the presence of two disynaptic basins in each region. This behaviour accounts for the high activation energy associated with the imine N–C and ketene C–C bond rotations, which prevent the *E*/*Z* imine and *cis*/*trans* ketene isomerisations.

Along the ring-closure step, formation of the new C–C single bond takes place at a C–C length of 2.079 Å, through the C-to-C coupling of two *pseudoradical centers* generated in previous phases.[33] Along this step, no specific imine N–C and ketene C–C bond rotations take place along the formation of the second C–C single bond, ruling out any torquoelectronic effect.[4] In addition, ELF population analysis of the N–C single bond formed along the first step of the reaction indicates that it does not participate in the ring-closure process. This behaviour, which is contrary to that observed in the electrocyclic aperture of cyclobutene **5**,[8b] makes it possible to reject any electrocyclic process along the second step of KI-S reactions.[4]

The present theoretical study together with the recent study devoted to the selectivity in the formation of β- *vs.* δ-lactams in KI-S reactions using unsaturated imines[15] allows us to reject these theoretical studies based on the FMO theory, in which HOMO/LUMO interactions along the nucleophilic attack of the imines on the ketenes and torquoelectronic effects along a conrotatory *pseudo*-electrocyclic reaction control the *cis*/*trans* stereoselectivity in the formation of β-lactams.

Acknowledgements

This work has been supported by the Ministerio de Economía y Competitividad of the Spanish Government, project CTQ2013-45646-P. M. R.-G. thanks the Ministerio de Economía y Competitividad for a pre-doctoral contract (BES-2014-068258).

References

1 (*a*) R. Southgate and S. Elson, *The Chemistry of Organic Natural Products*, Springer-Verlag, Wien, 1985, vol. 47; (*b*) R. Southgate, C. Branch, S. Coulton and E. Hunt, *Recent Progress in the Chemical Synthesis of Antibiotics and Related Microbial Products*, Springer-Verlag, Berlin, 1993, vol. 2; (*c*) R. Southgate, *Contemp. Org. Synth.*, 1994, **1**, 417.

2 (*a*) H. Staudinger, *Justus Liebigs Ann. Chem.*, 1907, **356**, 51; (*b*) T. T. Tidwell, *Ketenes*, John Wiley & Sons, New York, 1995.

3 (*a*) *The Organic Chemistry of β-Lactams*, ed. G. I. Georg, Verlag Chemie, New York, 1993; (*b*) C. Palomo, J. M. Aizpurua, I. Ganboa and M. Oiarbide, *Eur. J. Org. Chem.*, 1999, 3223; (*c*) G. S. Singh, *Tetrahedron*, 2003, **59**, 7631; (*d*) C. Palomo, J. M. Aizpurua, I. Ganboa and M. Oiarbide, *Curr. Med. Chem.*, 2004, **11**, 1837; (*e*) B. Alcaide, P. Almendros and C. Aragoncillo, *Chem. Rev.*, 2007, **107**, 4437; (*f*) A. Brandi, S. Cicchi and F. M. Cordero, *Chem. Rev.*, 2008, **108**, 3988.

4 F. P. Cossío, A. Arrieta and M. A. Sierra, *Acc. Chem. Res.*, 2008, **41**, 925.

5 (*a*) J. A. Sordo, J. González and T. L. Sordo, *J. Am. Chem. Soc.*, 1992, **114**, 6249; (*b*) F. P. Cossío, J. M. Ugalde, X. López, B. Lecea and C. Palomo, *J. Am. Chem. Soc.*, 1993, **115**, 995; (*c*) F. P. Cossío, A. Arrieta, B. Lecea and J. M. Ugalde, *J. Am. Chem. Soc.*, 1994, **116**, 2085; (*d*) A. Arrieta, B. Lecea and F. P. Cossío, *J. Org. Chem.*, 1998, **63**, 5869; (*e*) A. Arrieta, F. P. Cossío, I. Fernández, M. Gómez-Gallego, B. Lecea, M. J. Mancheno and M. A. Sierra, *J. Am. Chem. Soc.*, 2000, **122**, 11509; (*f*) A. Venturini and J. González, *J. Org. Chem.*, 2002, **67**, 9089; (*g*) B. K. Banik, B. Lecea, A. Arrieta, A. de Cózar and F. P. Cossío, *Angew. Chem., Int. Ed.*, 2007, **46**, 3028; (*h*) I. Fernández, M. A. Sierra, M. J. Mancheno, M. Gómez-Gallego and F. P. Cossío, *J. Am. Chem. Soc.*, 2008, **130**, 13892.

6 (*a*) H. W. Moore and G. Hughes, *Tetrahedron Lett.*, 1982, **23**, 4003; (*b*) W. T. Brady and C. H. Shieh, *J. Org. Chem.*, 1983, **48**, 2499.

7 (*a*) W. Kirmse, N. G. Rondan and K. N. Houk, *J. Am. Chem. Soc.*, 1984, **106**, 7989; (*b*) C. W. Jefford, G. Bernardelli, Y. Wang, D. C. Spellmeyer, A. Buda and K. N. Houk, *J. Am. Chem. Soc.*, 1992, **114**, 1157.

8 (*a*) V. Polo, J. Andrés, S. Berski, L. R. Domingo and B. Silvi, *J. Phys. Chem. A*, 2008, **112**, 7128; (*b*) J. Andrés, S. Berski, L. R. Domingo, V. Polo and B. Silvi, *Curr. Org. Chem.*, 2011, **15**, 3566; (*c*) J. Andrés, P. González-Navarrete and V. S. Safont, *Int. J. Quantum Chem.*, 2014, **114**, 1239.

9 A. D. Becke and K. E. Edgecombe, *J. Chem. Phys.*, 1990, **92**, 5397.

10 (*a*) A. Savin, A. D. Becke, J. Flad, R. Nesper, H. Preuss and H. G. Vonschnering, *Angew. Chem., Int. Ed.*, 1991, **30**, 409; (*b*) B. Silvi and A. Savin, *Nature*, 1994, **371**, 683; (*c*) A. Savin, B. Silvi and F. Colonna, *Can. J. Chem.*, 1996, **74**, 1088; (*d*) A. Savin, R. Nesper, S. Wengert and T. F. Fassler, *Angew. Chem., Int. Ed. Engl.*, 1997, **36**, 1809.

11 K. Fukui, *J. Phys. Chem.*, 1970, **74**, 4161.

12 K. N. Houk, J. González and Y. Li, *Acc. Chem. Res.*, 1995, **28**, 81.

13 F. A. Carey and R. J. Sundberg, *Advanced Organic Chemistry. Part A: Structure and Mechanisms*, Springer, New York, 2000.

14 R. B. Woodward and R. Hoffmann, *Angew. Chem., Int. Ed. Engl.*, 1969, **8**, 781.

15 L. R. Domingo and J. A. Sáez, *RSC Adv.*, 2014, **4**, 58559.

16 R. G. Parr, L. Von Szentpaly and S. Liu, *J. Am. Chem. Soc.*, 1999, **121**, 1922.

17 (*a*) L. R. Domingo, E. Chamorro and P. Pérez, *J. Org. Chem.*, 2008, **73**, 4615; (*b*) L. R. Domingo and P. Pérez, *Org. Biomol. Chem.*, 2011, **9**, 7168.

18 H. W. Moore, G. Hughes, K. Srinivasachar, M. Fernandez, N. V. Nguyen, D. Schoon and A. Tranne, *J. Org. Chem.*, 1985, **50**, 4231.

19 Y. Zhao and D. G. Truhlar, *J. Phys. Chem. A*, 2004, **108**, 6908.

20 W. J. Hehre, L. Radom, P. v. R. Schleyer and J. A. Pople, *Ab initio Molecular Orbital Theory*, Wiley, New York, 1986.

21 (*a*) H. B. Schlegel, *J. Comput. Chem.*, 1982, **3**, 214; (*b*) *Modern Electronic Structure Theory*, ed. H. B. Schlegel and D. R. Yarkony, World Scientific Publishing, Singapore, 1994.
22 (*a*) C. González and H. B. Schlegel, *J. Phys. Chem.*, 1990, **94**, 5523; (*b*) C. González and H. B. Schlegel, *J. Chem. Phys.*, 1991, **95**, 5853.
23 (*a*) J. Tomasi and M. Persico, *Chem. Rev.*, 1994, **94**, 2027; (*b*) B. Y. Simkin and I. Sheikhet, *Quantum Chemical and Statistical Theory of Solutions – Computational Approach*, Ellis Horwood, London, 1995.
24 (*a*) E. Cances, B. Mennucci and J. Tomasi, *J. Chem. Phys.*, 1997, **107**, 3032; (*b*) M. Cossi, V. Barone, R. Cammi and J. Tomasi, *Chem. Phys. Lett.*, 1996, **255**, 327; (*c*) V. Barone, M. Cossi and J. Tomasi, *J. Comput. Chem.*, 1998, **19**, 404.
25 (*a*) A. E. Reed, R. B. Weinstock and F. Weinhold, *J. Chem. Phys.*, 1985, **83**, 735; (*b*) A. E. Reed, L. A. Curtiss and F. Weinhold, *Chem. Rev.*, 1988, **88**, 899.
26 S. Noury, X. Krokidis, F. Fuster and B. Silvi, *Comput. Chem.*, 1999, **23**, 597.
27 M. J. Frisch, *et al.*, *Gaussian 09, Revision A.02*, Gaussian Inc, Wallingford CT, 2009.
28 (*a*) R. G. Parr and R. G. Pearson, *J. Am. Chem. Soc.*, 1983, **105**, 7512; (*b*) R. G. Parr and W. Yang, *Density Functional Theory of Atoms and Molecules*, Oxford University Press, New York, 1989.
29 W. Kohn and L. J. Sham, *Phys. Rev.*, 1965, **140**, 1133.
30 Y. Zhao and D. G. Truhlar, *Theor. Chem. Acc.*, 2008, **120**, 215.
31 A. Savin, *J. Chem. Sci.*, 2005, **117**, 473.
32 B. Silvi, *J. Mol. Struct.*, 2002, **614**, 3.
33 L. R. Domingo, *RSC Adv.*, 2014, **4**, 32415.